Letter

Genus drop in hyperelliptic Feynman integrals

Robin Marzucca[,1] Andrew J. McLeod[,2,3] Ben Page,[2] Sebastian Pögel[,4] and Stefan Weinzierl[4]

[1]*Physik-Institut, Universität Zürich, Winterthurerstrasse 190, 8057 Zürich, Switzerland*
[2]*CERN, Theoretical Physics Department, 1211 Geneva 23, Switzerland*
[3]*Mani L. Bhaumik Institute for Theoretical Physics, Department of Physics and Astronomy,*
UCLA, Los Angeles, California 90095, USA
[4]*PRISMA Cluster of Excellence, Institut für Physik, Staudinger Weg 7,*
Johannes Gutenberg-Universität Mainz, D-55099 Mainz, Germany

The maximal cut of the nonplanar crossed box diagram with all massive internal propagators was long ago shown to encode a hyperelliptic curve of genus 3 in momentum space. Surprisingly, in Baikov representation, the maximal cut of this diagram only gives rise to a hyperelliptic curve of genus 2. To show that these two representations are in agreement, we identify a hidden involution symmetry that is satisfied by the genus 3 curve, which allows it to be algebraically mapped to the curve of genus 2. We then argue that this is just the first example of a general mechanism by means of which hyperelliptic curves in Feynman integrals can drop from genus g to $\lceil g/2 \rceil$ or $\lfloor g/2 \rfloor$. We find an algorithm to test for the presence of genus drop, and highlight further instances of this mechanism in Feynman integrals.

Introduction. The immense amount of data collected at the LHC provides us with a unique opportunity to search for hints of new physics beyond the Standard Model. In the coming years, a number of observables will be measured with percent-level precision that probe the properties of the Higgs and electroweak symmetry breaking. Making use of these measurements crucially requires Standard Model predictions with the same level of precision. This presents an immense theoretical challenge, especially near the electroweak scale where finite-mass effects related to top quarks, vector bosons, and the Higgs become relevant. Even at two loops, the scattering amplitudes that encode these finite-mass corrections remain well beyond the state of the art.

The difficulty of computing amplitudes involving massive virtual particles comes in large part from the types of special functions these amplitudes evaluate to. While a great deal of technological progress has been made by focusing on amplitudes that evaluate to multiple polylogarithms [1–19], amplitudes with internal masses are known to give rise to integrals over nontrivial curves and K3 surfaces already at two loops [20–22]. It is thus important to characterize the types of integrals that can appear, and the simplest class of special functions a given Feynman integral can be evaluated in terms of.

One of the types of functions that are known to arise starting at two loops are integrals over hyperelliptic curves [22–24]. Hyperelliptic curves are algebraic curves of genus $g > 1$ whose defining equation takes the form $y^2 = P(z)$, for some polynomial $P(z)$ of degree $(2g + 1)$ or $(2g + 2)$. They generalize elliptic curves, whose defining equation takes the same form when $g = 1$. Feynman diagrams that give rise to elliptic curves have received significant attention in recent years [20,25–66], as have diagrams that give rise to integrals over higher-dimensional varieties [39,55,67–80]. In contrast, Feynman diagrams that give rise to curves with genus $g > 1$ have received little attention. A more in-depth study of these integrals is long overdue.

The types of integrals that appear in Feynman diagrams can be diagnosed by studying their maximal cut, in which all propagators are put on-shell. In this paper, we focus on diagrams whose maximal cut is given by a one-fold integral of the form

$$\int \frac{dz N(z)}{\sqrt{P(z)}}, \qquad (1)$$

where $N(z)$ and $P(z)$ are polynomials of z [81], as these diagrams are expected to give rise to iterated integrals involving differential one-forms related to the curve $y^2 = P(z)$ [82]. In this paper we highlight that the curve one associates with a given Feynman diagram in this way can have different genus depending on the chosen integral representation. We illustrate this with the example of the massive nonplanar crossed box diagram shown in Fig. 1;
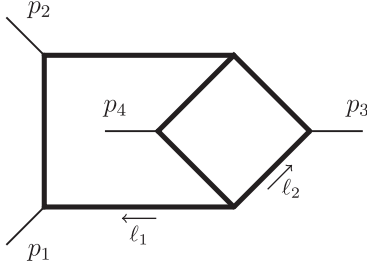
FIG. 1. The nonplanar crossed box diagram, with massive internal propagators.

while its maximal cut in momentum space involves a curve of genus 3 [24], in Baikov representation it involves a curve of genus 2.

In order to make sense of this discrepancy, we analyze the properties of these curves in more detail. We find that the genus 3 curve has an extra involution symmetry, which can be made manifest through a change of variables that brings its defining equation into a form that only depends on z^2 (whereupon the action of the involution is simply $z \to -z$). Through the change of variables $w = z^2$, this genus 3 curve can then be mapped to a curve of genus 2 that is isomorphic to the curve that appears in the Baikov representation.

More generally, we show that any genus g hyperelliptic curve that enjoys an extra involution symmetry can be related to a pair of hyperelliptic curves of genus $\lceil \frac{g}{2} \rceil$ and $\lfloor \frac{g}{2} \rfloor$. After constructing the explicit mappings between these curves, we present an algorithm for detecting the existence of such an involution and constructing the change of variables that makes this involution manifest. Finally, we describe the implications that this extra involution has for the period matrices of these hyperelliptic curves, and show that the entries of this matrix satisfy linear relations among themselves. We conclude by pointing to additional examples of Feynman integrals whose maximal cuts in momentum space experience similar genus drops.

The nonplanar crossed box. The main example we focus on in this paper is the nonplanar crossed box diagram with equal internal masses in four dimensions, shown in Fig. 1. It can be written as

$$I^{\text{NPCB}} = \int \frac{\mathrm{d}^4 \ell_1}{i\pi^2} \frac{\mathrm{d}^4 \ell_2}{i\pi^2} \frac{1}{\prod_{i=1}^{7} D_i}, \qquad (2)$$

where the propagators are given by

$$D_1 = \ell_1^2 - m^2, \qquad D_2 = (\ell_1 - p_1)^2 - m^2,$$
$$D_3 = (\ell_1 - p_1 - p_2)^2 - m^2, \qquad D_4 = \ell_2^2 - m^2,$$
$$D_5 = (\ell_2 - p_3)^2 - m^2, \qquad D_6 = (\ell_1 + \ell_2)^2 - m^2,$$
$$D_7 = (\ell_1 + \ell_2 - p_1 - p_2 - p_3)^2 - m^2. \qquad (3)$$

With the external momenta massless $p_i^2 = 0$, the integral depends on three kinematic variables, $s = (p_1 + p_2)^2$, $t = (p_2 + p_3)^2$, and m^2.

In [23,24], the maximum cut of this diagram was computed directly in momentum space, and was found to take the form

$$\text{MaxCut}_{\text{MOM}}(I^{\text{NPCB}}) \sim \int \frac{\mathrm{d}z \, z}{\sqrt{P_8(z)}}, \qquad (4)$$

where $P_8(z)$ is a polynomial of degree eight in the variable $z = \text{tr}_-(p_4 p_2 \ell_1 p_1)/s^2$ whose coefficients depend on s, t, and m^2 [83]. The maximal cut thus defines a period of a hyperelliptic curve of genus 3 [84]. This implies the full integral should be expressible in terms of iterated integrals involving one-forms related to the genus 3 curve defined by $P_8(z)$.

We can also compute the maximal cut of this integral using a loop-by-loop Baikov parametrization. In this representation, the maximal cut takes the form

$$\text{MaxCut}_{\text{LBL}}(I^{\text{NPCB}}) \sim \int \frac{\mathrm{d}z}{\sqrt{P_6(z)}}, \qquad (5)$$

where now the integration variable $z = (\ell_1 \cdot p_3)$ is an irreducible scalar product that was introduced when realizing the Baikov representation, and $P_6(z)$ is a degree-six polynomial in z. This form of the maximal cut therefore seems to imply that the nonplanar crossed box can be expressed in terms of iterated integrals involving one-forms related to a curve of genus 2. We verified that the Picard-Fuchs operator of the maximal cut on generic one-dimensional kinematic slices has order 4, consistent with a curve of genus 2.

This leaves us in a perplexing situation, as our expectation for the types of iterated integrals that will appear in the nonplanar crossed box depends on which representation of the integral we start from. The polynomials $P_6(z)$ and $P_8(z)$ define curves of different genus, between which there can exist no birational transformation. Their explicit forms are

$$P_6(z) = s(2z(s+2z) - 3m^2 s)(m^2 s + 2z(s+2z))(s(s+t+2z)^2 - 4m^2 t(s+t)),$$
$$P_8(z) = (s+t)^2(t^2 m^2 + s^2 z(sz+t))(m^2(s+t)^2 + s^2 z(sz+s+t))$$
$$\times (s^2 z m^2(-3s^3 z + s^2(2tz+t) + st^2(2z+3) + 2t^3) + t^2(m^2)^2(s+t)^2 + s^4 z^2(sz+t)(sz+s+t)), \qquad (6)$$

A mechanism for genus drop. The resolution of this apparent discrepancy turns out to be related to the group of automorphisms that we can associate to the genus 3 curve. In particular, this curve has an additional involution symmetry that allows it to be algebraically mapped to a pair of curves of lower genus. To see how this comes about, we now review some properties of hyperelliptic curves.

A hyperelliptic curve of genus g is defined by the (affine) equation

$$\mathcal{H}: y^2 = P(z), \qquad (7)$$

where $P(z)$ is a polynomial of degree $2g + 1$ or $2g + 2$. We denote the roots of $P(z)$ as $\alpha_i \in \mathbb{P}^1$, and without loss of generality we specialize to the case where the degree is $2g + 2$. We can find new, equivalent representations of the curve via Möbius transformations. For $\gamma = \left(\begin{smallmatrix} a & b \\ c & d \end{smallmatrix}\right) \in \mathbb{C}^{2\times2}$ with $\det \gamma \neq 0$, the new representation of the curve has the form $\mathcal{H}: \hat{y}^2 = \hat{P}(\hat{z})$, where

$$z = \gamma[\hat{z}] \equiv \frac{a\hat{z} + b}{c\hat{z} + d}, \qquad y = \hat{y} \frac{1}{(c\hat{z} + d)^{2g+2}}, \qquad (8)$$

and

$$\hat{P}(\hat{z}) = (c\hat{z} + d)^{2g+2} P(\gamma[\hat{z}]), \qquad (9)$$

with roots $\hat{\alpha}_i = \gamma^{-1}[\alpha_i]$.

We consider the automorphism group $\text{Aut}(\mathcal{H})$ of the curve $\mathcal{H}$ [85]. For (hyper)elliptic curves, this group always includes the involution

$$e_0: \quad y \to -y. \qquad (10)$$

The reduced automorphism group $\overline{\text{Aut}}(\mathcal{H}) \equiv \text{Aut}(\mathcal{H})/\langle e_0 \rangle$ consists of Möbius transformations that permute the roots of the polynomial $P(z)$ [86,87].

A hyperelliptic curve is said to possess an extra involution $e_1 \in \overline{\text{Aut}}(\mathcal{H})$ if there exists a Möbius transformation, such that

$$\hat{P}(\hat{z}) = Q(\hat{z}^2) \equiv c(\hat{z}^2 - \hat{\alpha}_1^2)...(\hat{z}^2 - \hat{\alpha}_{g+1}^2), \qquad (11)$$

where $c \in \mathbb{C}$ is a constant [88]. The roots thus come in pairs $\pm \hat{\alpha}_i$, and the extra involution acts as

$$e_1: \quad \hat{z} \to -\hat{z}. \qquad (12)$$

We can then define another involution by composition,

$$e_2 = e_1 \circ e_0: \quad (\hat{y}, \hat{z}) \to (-\hat{y}, -\hat{z}). \qquad (13)$$

To our curve $\mathcal{H}$, we can associate the two curves

$$\mathcal{H}_1: \quad v_1^2 = Q(w) = c(w - \hat{\alpha}_1^2)...(w - \hat{\alpha}_{g+1}^2),$$
$$\mathcal{H}_2: \quad v_2^2 = wQ(w) = cw(w - \hat{\alpha}_1^2)...(w - \hat{\alpha}_{g+1}^2). \qquad (14)$$

We can recover $\mathcal{H}$ via the maps

$$\rho_1: (v_1, w) \to (\hat{y}, \hat{z}^2), \qquad \rho_2: (v_2, w) \to (\hat{y}\hat{z}, \hat{z}^2), \qquad (15)$$

which are invariant under e_1 and e_2, respectively. From the degree of their defining polynomial in w, the curves $\mathcal{H}_1$ and $\mathcal{H}_2$ have genera $g_1 = \lfloor \frac{g}{2} \rfloor$ and $g_2 = \lfloor \frac{g+1}{2} \rfloor = \lceil \frac{g}{2} \rceil$. Note that, in addition to the roots at $\hat{\alpha}_i^2$, the curve $\mathcal{H}_2$ has a branch point at 0; moreover, depending on whether $\lfloor \frac{g}{2} \rfloor$ is even or odd, either $\mathcal{H}_1$ or $\mathcal{H}_2$ will have a branch point at ∞.

In the Supplementary Material [89], we provide a reference implementation of an algorithm that tests for the presence of an extra involution, and if it exists, provides the required transformation γ.

Genus drop in the maximal cut. We now illustrate how this genus drop mechanism works for the case of the nonplanar crossed box. Starting from a general Möbius transformation $z = \gamma_1[\hat{z}]$ and solving for its parameters such that the coefficients of odd power monomials in $\hat{z}$ vanish, we find a transformation

$$\gamma_1 = \begin{pmatrix} 1 & -1 \\ r & r \end{pmatrix}, \qquad z = \gamma_1[\hat{z}] = \frac{1}{r} \frac{\hat{z} - 1}{\hat{z} + 1}, \qquad (16)$$

where $r = \sqrt{s^3/(m^2 t(s + t))}$. The polynomial

$$Q_4(\hat{z}^2) = (r\hat{z} + r)^8 P_8 \left(\frac{1}{r} \frac{\hat{z} - 1}{\hat{z} + 1} \right), \qquad (17)$$

then only depends on powers of $\hat{z}^2$. [Note that $Q_4(\hat{z}^2)$ is of degree 4 in $\hat{z}^2$, and therefore of degree 8 in $\hat{z}$.] In this case, the extra involution maps

$$e_1[\text{tr}_-(p_4 p_2 \ell_1 p_1)] = \text{tr}_+(p_4 p_2 \ell_1 p_1). \qquad (18)$$

Hence, the extra involution can be associated to parity.

Following the notation of the previous section, we define $w \equiv \hat{z}^2$, $v_1 \equiv y$, and $v_2 \equiv yw$. We can then associate two curves with the original genus 3 curve; the elliptic curve

$$v_1^2 = Q_4(w), \qquad (19)$$

and the genus 2 hyperelliptic curve

$$v_2^2 = wQ_4(w) \equiv Q_5(w). \qquad (20)$$

Comparing the period matrices of the latter curve and the curve found from the Baikov representation, we see that they generate the same lattice. The curves are therefore isomorphic. Equivalently, we find that they have the same absolute invariants (as defined by Clebsch or Igusa [90–92]), which
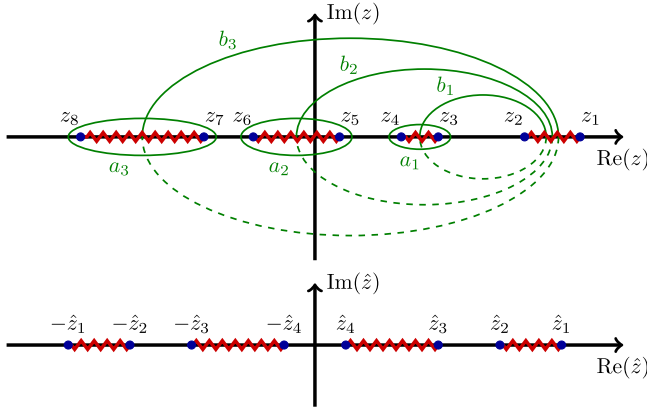
FIG. 2. The upper figure shows the branch cuts of a $g = 3$ hyperelliptic curve and a basis of integration contours. The lower figure illustrates how roots pair up when this curve has an extra involution and can be put in the form of Eq. (11).

characterize curves of genus 2 [93]. We find the explicit transformation,

$$\gamma_2 = \begin{pmatrix} a & b \\ c & d \end{pmatrix} = \frac{m^4}{\sqrt[3]{2s^5(s+t)}} \begin{pmatrix} 1 & \frac{s+t}{2m^2} - \sqrt{\frac{(s+t)t}{sm^2}} \\ 1 & \frac{s+t}{2m^2} + \sqrt{\frac{(s+t)t}{sm^2}} \end{pmatrix}, \quad (21)$$

relating these curves via

$$(cw + d)^6 Q_5(\gamma_2[w]) = P_6(w). \quad (22)$$

Additional period relations. The presence of the extra involution also has consequences for the periods of a hyperelliptic curve. We recall that the periods of a genus g curve correspond to the different possible pairings between a basis of g holomorphic differentials ω_i and $2g$ integration contours Γ_j. For a hyperelliptic curve of genus g defined by the polynomial $P_{2g+2}(z)$, a basis of holomorphic differentials is given by $z^{i-1}dz/\sqrt{P_{2g+2}(z)}$ for $i = 1, \dots, g$. An example of a basis of contours for a genus 3 hyperelliptic curve with real roots is shown in Fig. 2. The entries of the $(g \times 2g)$-dimensional period matrix $\mathcal{P}$ of the curve $\mathcal{H}$ are given by

$$\mathcal{P}_{ij} = \int_{\Gamma_j} \frac{z^{i-1}dz}{\sqrt{P_{2g+2}(z)}}, \quad (23)$$

where $i \in \{1, \dots, g\}$, $j \in \{1, \dots, 2g\}$.

Assume that $\mathcal{H}$ has an extra involution, which can be made manifest using the coordinate transformation $z = \frac{a\hat{z}+b}{c\hat{z}+d}$. Then,

$$\int \frac{dz z^{i-1}}{\sqrt{P_{2g+2}(z)}} \propto \int \frac{dw(\sqrt{w} \pm \frac{b}{a})^{i-1}(\sqrt{w} \pm \frac{d}{c})^{g-(i-1)}}{\sqrt{w Q_{g+1}(w)}}, \quad (24)$$

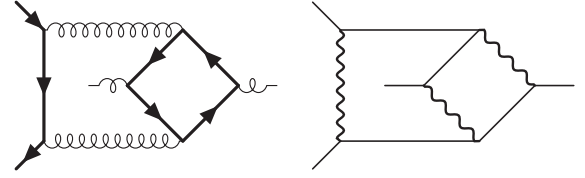FIG. 3. Examples of hyperelliptic Feynman integrals in which genus drop via an extra involution can be observed. These integrals contribute to $gg \to t\bar{t}$ with a top loop, and Møller scattering $e^-e^- \to e^-e^-$ with the exchange of three Z bosons. Thick lines denote massive particles.

where $\hat{z} = \pm\sqrt{w}$. By expanding out Eq. (24), all periods of $\mathcal{H}$ are expressible as linear combinations of the periods of subcurves $\mathcal{H}_1$ and $\mathcal{H}_2$ [94]. More generally, we can find matrices $M_\omega \in \mathbb{C}^{g \times g}$ and $M_\Gamma \in \mathbb{Z}^{2g \times 2g}$ such that

$$M_\omega^t \mathcal{P} M_\Gamma = \begin{pmatrix} \mathcal{P}_1 & 0 \\ 0 & \mathcal{P}_2 \end{pmatrix}, \quad (25)$$

where $\mathcal{P}_1$ and $\mathcal{P}_2$ are period matrices of $\mathcal{H}_1$ and $\mathcal{H}_2$. There must correspondingly be $4 \times \lfloor g/2 \rfloor \times \lceil g/2 \rceil$ relations between the periods of the curve defined by $P_{2g+2}(z)$ [95].

Further examples. Although we have mainly focused in this paper on the nonplanar crossed box with equal internal masses, genus drop can be observed in phenomenologically-relevant examples involving different masses. For example, Fig. 3 depicts one diagram that contributes to $t\bar{t}$ production and another that contributes to Møller scattering. The maximum cut of both diagrams involve curves of genus 3 in momentum space that enjoy an extra involution symmetry and can be mapped to curves of genus 2.

In fact, genus drop can be also be seen in an infinite number of necklace diagrams, as studied in [96]. For instance, when all of the beads in these necklaces are taken to be bubbles and all but two external particles are taken to be soft, we land on the class of "broken" necklace graphs depicted in Fig. 4. These integrals can be shown to give rise to integrals over hyperelliptic curves of any genus, when each propagator is assigned a different mass [97]. In particular, a naive parametrization of these diagrams in momentum space naturally give rise to a curve of genus
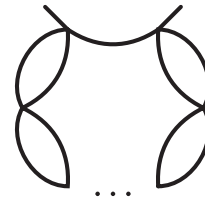

FIG. 4. A class of (broken) necklace diagrams, which can be seen to drop from genus $2L - 3$ to $L - 1$ at all loop orders, when all propagators are assigned different masses.

$2L - 3$; however, by going to Baikov, these curves can be seen to drop to genus $\lceil \frac{2L-3}{2} \rceil = L - 1$.

The genus drop mechanism is also relevant in special kinematic limits. For instance, a further involution symmetry appears in the equal-mass nonplanar crossed box diagram when $s = -2t$. In this limit there is a permutation symmetry that exchanges $p_1 \leftrightarrow p_2$, and the curve becomes

$$y^2 = 8t^2(2\hat{z}^2 - m^2 t)(4\hat{z}^2 - 2m^2 t - t^2)(4\hat{z}^2 + 6m^2 t - t^2),$$

with $\hat{z} = z - \frac{t}{2}$. This makes it evident that the maximal cut of this diagram drops from genus 2 to genus 1 in this limit. This is consistent with the Picard-Fuchs operator associated with this integral, which we also observe to drop from order 4 to order 2 when $s = -2t$.

Conclusion. In this paper we have studied Feynman diagrams that give rise to integrals over hyperelliptic curves, and highlighted the fact that different integral representations of these diagrams can lead to curves with different genera. We have studied a number of hyperelliptic integrals exhibiting this phenomenon, highlighting the nonplanar double box as the first known four-dimensional genus 2 example at two loops, as well as the infinite class of necklace diagrams that demonstrate the ubiquity of genus drop in quantum field theory. Importantly, genus drop represents a significant simplification in the types of functions that these diagrams are expected to evaluate to. In all of our examples, we have observed that this discrepancy in genus can be explained by the presence of an extra involution symmetry that algebraically maps the higher-genus curve to the lower-genus one. We expect that such extra involutions in the momentum representation can follow from discrete Lorentz symmetries (spacetime parity or time reversal). We also find an algorithm to detect when an extra involution exists, and showed that this symmetry leads to linear relations among the periods of the corresponding curve. We expect that these insights into the geometry of

Feynman integrals will have important impact on future computations of hyperelliptic scattering amplitudes.

While it is important to be able to diagnose which class of special functions a given Feynman integral is expected to be expressible in terms of, given the ubiquity of hyperelliptic Feynman integrals, it is even more essential to develop the technology for working with these classes of functions. Despite remarkable recent progress on iterated integrals involving elliptic curves (see [98] for an overview), much less technology has been developed for iterated integrals over hyperelliptic curves (however, for recent work see [99–101]). The nonplanar crossed box with equal internal masses represents an ideal example on which to develop such technology, given that—as we have newly shown—it involves only a curve of genus 2 [102].

Having identified a novel class of simplifications that can occur in hyperelliptic Feynman integrals, it is natural to wonder whether analogous simplifications can occur in Feynman integrals that involve integrals over more general varieties, such as curves that are not hyperelliptic or higher-dimensional Calabi-Yaus. One way to search for evidence of such simplifications would be to look for unexpected relations between entries of the period matrix. We leave this enticing possibility to future work.

[1] K.-T. Chen, Bull. Am. Math. Soc. **83**, 831 (1977).

[2] A. B. Goncharov, Adv. Math. **114**, 197 (1995).

[3] A. B. Goncharov, Math. Res. Lett. **5**, 497 (1998).

[4] E. Remiddi and J. Vermaseren, Int. J. Mod. Phys. A **15**, 725 (2000).

[5] J. M. Borwein, D. M. Bradley, D. J. Broadhurst, and P. Lisonek, Trans. Am. Math. Soc. **353**, 907 (2001).

[6] S. Moch, P. Uwer, and S. Weinzierl, J. Math. Phys. (N.Y.) **43**, 3363 (2002).

[7] F. C. Brown, Ann. Sci. Ecole Norm. Sup. **42**, 371 (2009).

[8] A. B. Goncharov, M. Spradlin, C. Vergu, and A. Volovich, Phys. Rev. Lett. **105**, 151605 (2010).

[9] M. Deneufchâtel, G. H. E. Duchamp, V. H. N. Minh, and A. I. Solomon, in *Algebraic Informatics*, edited by F. Winkler (Springer Berlin Heidelberg, Berlin, Heidelberg, 2011), pp. 127–139.

[10] S. Caron-Huot, J. High Energy Phys. 12 (2011) 066.

[11] E. Panzer, Comput. Phys. Commun. **188**, 148 (2015), HyperInt is obtainable at arXiv:1403.3385.

[12] L. J. Dixon, J. Drummond, T. Harrington, A. J. McLeod, G. Papathanasiou, and M. Spradlin, J. High Energy Phys. 02 (2017) 137.

[13] J. L. Bourjaily, A. J. McLeod, M. von Hippel, and M. Wilhelm, J. High Energy Phys. 08 (2018) 184.

[14] S. Caron-Huot, L. J. Dixon, M. von Hippel, A. J. McLeod, and G. Papathanasiou, J. High Energy Phys. 07 (2018) 170.

[15] J. Drummond, J. Foster, Ö. Gürdoğan, and G. Papathanasiou, J. High Energy Phys. 03 (2019) 087.

[16] S. Caron-Huot, L. J. Dixon, F. Dulat, M. von Hippel, A. J. McLeod, and G. Papathanasiou, J. High Energy Phys. 08 (2019) 016.

[17] S. He, Z. Li, and C. Zhang, J. High Energy Phys. 03 (2021) 278.

[18] S. He, Z. Li, and Q. Yang, J. High Energy Phys. 12 (2021) 110; 05 (2022) 75.

[19] L. J. Dixon, O. Gurdogan, A. J. McLeod, and M. Wilhelm, J. High Energy Phys. 07 (2022) 153.

[20] A. Sabry, Nucl. Phys. **33**, 401 (1962).

[21] P. Lairez and P. Vanhove, Lett. Math. Phys. **113**, 37 (2023).

[22] C. F. Doran, A. Harder, E. Pichon-Pharabod, and P. Vanhove, arXiv:2302.14840.

[23] R. Huang and Y. Zhang, J. High Energy Phys. 04 (2013) 080.

[24] A. Georgoudis and Y. Zhang, J. High Energy Phys. 12 (2015) 086.

[25] D. J. Broadhurst, J. Fleischer, and O. V. Tarasov, Z. Phys. C **60**, 287 (1993).

[26] M. Caffo, H. Czyz, S. Laporta, and E. Remiddi, Nuovo Cimento Soc. Ital. Fis. **111A**, 365 (1998).

[27] S. Laporta and E. Remiddi, Nucl. Phys. **B704**, 349 (2005).

[28] S. Müller-Stach, S. Weinzierl, and R. Zayadeh, Commun. Num. Theor. Phys. **6**, 203 (2012).

[29] M. F. Paulos, M. Spradlin, and A. Volovich, J. High Energy Phys. 08 (2012) 072.

[30] S. Caron-Huot and K. J. Larsen, J. High Energy Phys. 10 (2012) 026.

[31] D. Nandan, M. F. Paulos, M. Spradlin, and A. Volovich, J. High Energy Phys. 05 (2013) 105.

[32] L. Adams, C. Bogner, and S. Weinzierl, J. Math. Phys. (N.Y.) **54**, 052303 (2013).

[33] L. Adams, C. Bogner, and S. Weinzierl, J. Math. Phys. (N.Y.) **54**, 052303 (2013).

[34] S. Bloch and P. Vanhove, J. Number Theory **148**, 328 (2015).

[35] E. Remiddi and L. Tancredi, Nucl. Phys. **B880**, 343 (2014).

[36] L. Adams, C. Bogner, and S. Weinzierl, J. Math. Phys. (N.Y.) **55**, 102301 (2014).

[37] L. Adams, C. Bogner, and S. Weinzierl, J. Math. Phys. (N.Y.) **56**, 072303 (2015).

[38] L. Adams, C. Bogner, and S. Weinzierl, J. Math. Phys. (N.Y.) **57**, 032304 (2016).

[39] S. Bloch, M. Kerr, and P. Vanhove, Adv. Theor. Math. Phys. **21**, 1373 (2017).

[40] E. Remiddi and L. Tancredi, Nucl. Phys. **B907**, 400 (2016).

[41] L. Adams, C. Bogner, A. Schweitzer, and S. Weinzierl, J. Math. Phys. (N.Y.) **57**, 122302 (2016).

[42] R. Bonciani, V. Del Duca, H. Frellesvig, J. M. Henn, F. Moriello, and V. A. Smirnov, J. High Energy Phys. 12 (2016) 096.

[43] A. von Manteuffel and L. Tancredi, J. High Energy Phys. 06 (2017) 127.

[44] L. Adams and S. Weinzierl, Commun. Num. Theor. Phys. **12**, 193 (2018).

[45] C. Bogner, A. Schweitzer, and S. Weinzierl, Nucl. Phys. **B922**, 528 (2017).

[46] J. Ablinger, J. Blümlein, A. De Freitas, M. van Hoeij, E. Imamoglu, C. G. Raab, C. S. Radu, and C. Schneider, J. Math. Phys. (N.Y.) **59**, 062305 (2018).

[47] D. Chicherin and E. Sokatchev, J. High Energy Phys. 04 (2018) 082.

[48] J. L. Bourjaily, A. J. McLeod, M. Spradlin, M. von Hippel, and M. Wilhelm, Phys. Rev. Lett. **120**, 121603 (2018).

[49] J. Broedel, C. Duhr, F. Dulat, and L. Tancredi, Phys. Rev. D **97**, 116009 (2018).

[50] L. Adams and S. Weinzierl, Phys. Lett. B **781**, 270 (2018).

[51] J. Broedel, C. Duhr, F. Dulat, B. Penante, and L. Tancredi, J. High Energy Phys. 08 (2018) 014.

[52] L. Adams, E. Chaubey, and S. Weinzierl, Phys. Rev. Lett. **121**, 142001 (2018).

[53] L. Adams, E. Chaubey, and S. Weinzierl, J. High Energy Phys. 10 (2018) 206.

[54] J. Broedel, C. Duhr, F. Dulat, B. Penante, and L. Tancredi, J. High Energy Phys. 01 (2019) 023.

[55] J. L. Bourjaily, A. J. McLeod, M. von Hippel, and M. Wilhelm, Phys. Rev. Lett. **122**, 031601 (2019).

[56] P. Mastrolia and S. Mizera, J. High Energy Phys. 02 (2019) 139.

[57] I. Hönemann, K. Tempest, and S. Weinzierl, Phys. Rev. D **98**, 113008 (2018).

[58] J. Broedel, C. Duhr, F. Dulat, B. Penante, and L. Tancredi, J. High Energy Phys. 05 (2019) 120.

[59] J. Broedel, C. Duhr, F. Dulat, R. Marzucca, B. Penante, and L. Tancredi, J. High Energy Phys. 09 (2019) 112.

[60] S. Abreu, M. Becchetti, C. Duhr, and R. Marzucca, J. High Energy Phys. 02 (2020) 050.

[61] L. G. J. Campert, F. Moriello, and A. Kotikov, J. High Energy Phys. 09 (2021) 072.

[62] H. Frellesvig, C. Vergu, M. Volk, and M. von Hippel, J. High Energy Phys. 05 (2021) 064.

[63] A. Kristensson, M. Wilhelm, and C. Zhang, Phys. Rev. Lett. **127**, 251603 (2021).

[64] R. Morales, A. Spiering, M. Wilhelm, Q. Yang, and C. Zhang, Phys. Rev. Lett. **131**, 041601 (2023).

[65] A. McLeod, R. Morales, M. von Hippel, M. Wilhelm, and C. Zhang, J. High Energy Phys. 05 (2023) 236.

[66] C. F. Doran, A. Y. Novoseltsev, and P. Vanhove, Mirroring Towers: Calabi-Yau Geometry of the Multiloop Feynman Sunset Integrals (to be published).

[67] S. Bloch, M. Kerr, and P. Vanhove, Compos. Math. **151**, 2329 (2015).

[68] J. L. Bourjaily, Y.-H. He, A. J. McLeod, M. von Hippel, and M. Wilhelm, Phys. Rev. Lett. **121**, 071603 (2018).

[69] J. L. Bourjaily, A. J. McLeod, C. Vergu, M. Volk, M. Von Hippel, and M. Wilhelm, J. High Energy Phys. 01 (2020) 078.

[70] A. Klemm, C. Nega, and R. Safari, J. High Energy Phys. 04 (2020) 088.

[71] C. Vergu and M. Volk, J. High Energy Phys. 07 (2020) 160.

[72] K. Bönisch, F. Fischbach, A. Klemm, C. Nega, and R. Safari, J. High Energy Phys. 05 (2021) 066.

[73] K. Bönisch, C. Duhr, F. Fischbach, A. Klemm, and C. Nega, J. High Energy Phys. 09 (2022) 156.

[74] S. Pögel, X. Wang, and S. Weinzierl, J. High Energy Phys. 09 (2022) 062.

[75] C. Duhr, A. Klemm, F. Loebbert, C. Nega, and F. Porkert, Phys. Rev. Lett. **130**, 041602 (2023).

[76] S. Pögel, X. Wang, and S. Weinzierl, Phys. Rev. Lett. **130**, 101601 (2023).

[77] S. Pögel, X. Wang, and S. Weinzierl, J. High Energy Phys. 04 (2023) 117.

[78] C. Duhr, A. Klemm, C. Nega, and L. Tancredi, J. High Energy Phys. 02 (2023) 228.

[79] Q. Cao, S. He, and Y. Tang, J. High Energy Phys. 04 (2023) 072.

[80] A. J. McLeod and M. von Hippel, arXiv:2306.11780.

[81] More specifically, we consider holomorphic integrands, which implies that the degree of $N(z)$ should satisfy $3 + 2 \deg N \le \deg P$.

[82] Note that Feynman integrals will also in general depend on the integral geometries associated with the maximal cut of their subtopologies.

[83] We define $\mathrm{tr}_\pm(abcd) \equiv \mathrm{tr}(\frac{1 \pm \gamma_5}{2} \not a \not b \not c \not d)$.

[84] This genus can also be confirmed by feeding the seven on-shell equations directly into SINGULAR [103].

[85] Consider the field of rational functions on the curve, $\mathbb{C}(y, z)$: rational functions of y and z such that y satisfies equation (7). Viewing $\mathbb{C}(y, z)$ as a field extension of $\mathbb{C}$ we can consider the group of automorphisms of this extension: $\mathrm{Aut}(\mathbb{C}(y, z)\mathbb{C})$, which is $\mathrm{Aut}(\mathcal{H})$. This is the set of automorphisms of $\mathbb{C}(y, z)$ that act as the identity on $\mathbb{C}$.

[86] J. Gutierrez, D. Sevilla, and T. Shaska, Lect. Notes Comput. Sci. **13**, 109 (2005).

[87] T. Shaska, Communications in algebra **42**, 4110 (2014).

[88] If a Möbius transformation exists to bring a curve into the form of equation (11), it will not be unique; alternate transformations exist that lead to the same projective curve in different affine charts.

[89] See Supplemental Material at http://link.aps.org/supplemental/10.1103/PhysRevD.109.L031901, which provides a *Mathematica* package with a reference implementation.

[90] J. ichi Igusa, Ann. Math. **72**, 612 (1960).

[91] A. Clebsch and P. Gordan, Thesaurus Math. **7** (1967).

[92] L. Beshaj, R. Hidalgo, S. Kruk, A. Malmendier, S. Quispe, and T. Shaska, Contemp. Math. **703**, 83 (2018).

[93] For curves of genus 3 defined over a field of characteristic 0, similar invariants were found by Shioda [87,104]. We include code for calculating these genus 2 and genus 3 absolute invariants in the Supplementary Material [89].

[94] In the example of the nonplanar crossed box, the maximal cut from equation (4) gets mapped by (16) to a linear combination of only genus 2 periods, since all non-integer powers of w drop out of the numerator.

[95] This reflects the fact that the Jacobian variety $\mathrm{Jac}(\mathcal{H})$, which corresponds to the $2g$ dimensional lattice spanned by the column vectors of $\mathcal{P}$, is in this case isogenous to $\mathrm{Jac}(\mathcal{H}_1) \times \mathrm{Jac}(\mathcal{H}_2)$ [86,105].

[96] T. Regge, E. R. Speer, and M. J. Westwater, Fortschr. Phys. **20**, 365 (1972).

[97] S. Abreu, A. Behring, A. J. McLeod, and B. Page (to be published).

[98] J. L. Bourjaily et al., arXiv:2203.07088.

[99] B. Enriquez and F. Zerbini, arXiv:2110.09341.

[100] B. Enriquez and F. Zerbini, arXiv:2212.03119.

[101] E. D'Hoker, M. Hidding, and O. Schlotterer, arXiv:2306.08644.

[102] Notably, the double box integral was also recently shown to be hyperelliptic for external kinematics in more than four dimensions [22]; however, the double box exhibits much more kinematic complexity, making it a less-than-ideal example.

[103] W. Decker, G.-M. Greuel, G. Pfister, and H. Schönemann, SINGULAR 4-2-1—A computer algebra system for polynomial computations, http://www.singular.uni-kl.de (2021).

[104] T. Shioda, Am. J. Math. **89**, 1022 (1967).

[105] G. Cardona, J. González, J.-C. Lario, and A. Rio, Manuscr. Math. **98**, 37 (1999).